ESRF	**Experiment title:** **In situ study of the active centres in the diiron phtalocyanine oxidation catalysts by Resonant Inelastic X-Ray Scattering and EXAFS.**	**Experiment number**: CH-2752
Beamline: ID26	**Date of experiment**: from: 12 Nov 2008 to: 19 Nov 2008	**Date of report**: 29/08/2010
Shifts: 18	**Local contact(s)**: Janine Grattage, Martin Sikora	*Received at ESRF:*

Names and affiliations of applicants (* indicates experimentalists):

Pavel Afanasiev *[a] Olga Safonova* [b] Jean-marc Millet* [a] Christophe Geantet* Alexander Sorokin*[a]

[a] Institut de Recherches sur la Catalyse et l'Environnement de Lyon IRCELYON, UMR 5256, CNRS – Université Lyon 1 2, av. A. Einstein, 69626 Villeurbanne Cedex (France)

[b] European Syncrotron Facility (ESRF) F-38043 Grenoble, France

Report:

Research context

Recent discovery of the intriguing ability of N-bridged diiron tert-tetrabutylphthalocyanine complex to oxidize methane at near-ambient temperatures using hydrogen peroxide as terminal oxidant unavoidably leads to the question of the origin of such remarkable properties [1,2]. The same system efficiently catalyzes oxidation of benzene [3] and alkyl aromatic compounds.[4]. This diiron complex with Fe-N-Fe structural unit belongs to the class of single atom bridged binuclear complexes comprising μ-oxo, μ-nitrido, and μ-carbido derivatives (Fig. 1) [5]. The Fe-N-Fe core with bridging nitrogen atom was shown to be essential for the catalytic activity of diiron μ-nitrido complex. Importantly, μ-oxo and μ-carbido dimers as well as mononuclear iron phthalocyanine complexes containing the same ligands were inactive in the low temperature oxidation of methane.

μ-Nitrido diiron phthalocyanine complex shares a similar structural feature, binuclear iron site, with enzyme capable of oxidizing methane, soluble methane monooxygenase (MMO).[6] Nevertheless, the coordination environments of these binuclear sites are quite different. The former is bonded to macrocyclic phthalocyanine ligands while the latter has non-heme glutamate carboxyl and histidine nitrogen ligands in its coordination environment. Moreover, high valent μ-nitrido diiron species with halogen ligands can be prepared in stable forms [7]. It is very important to identify which peculiar structural properties (e.g., spin states of iron and possible charge transfer between metal centers and ligands) in μ-nitrido dimers are responsible for their outstanding catalytic properties.

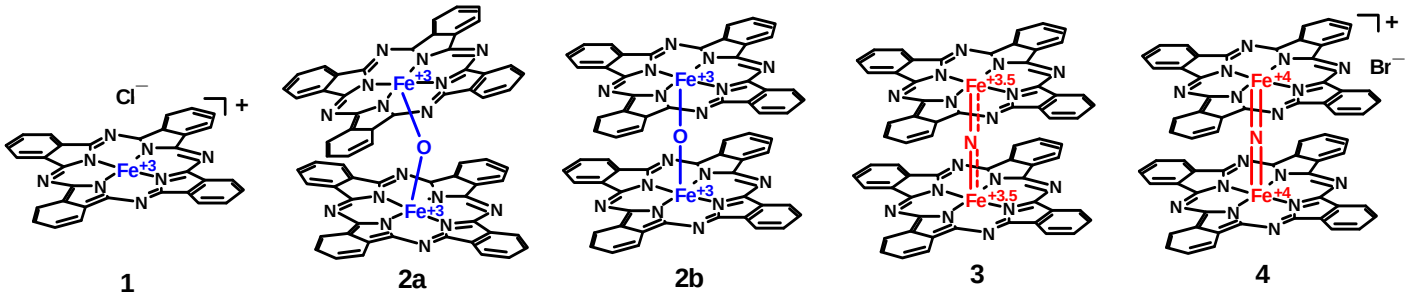

Figure 1. Complexes used in the study: Fe(III) phthalocyanine chloride (**1**), μ-oxo(1) Fe(III)-O-Fe(III) phthalocyanine (**2a**), μ-oxo(2) Fe(III)-O-Fe(III) phthalocyanine (**2b**), μ-nitrido Fe(III)-N-Fe(IV) phthalocyanine (**3**), and oxidized μ-nitrido Fe(IV)-N-Fe(IV) phthalocyanine bromide (**4**).

Physical methods based on X-ray absorption (XAS) and X-ray emission are of particular value for probing local and electronic structure around a specific transition metal atom. Such techniques have been successfully applied for characterization of non-heme [8,9,10] and heme [11,12, 13] iron-containing systems. They were used to study spin and oxidation states of iron in various inorganic solids. [14]. The aim of this study was to X-ray spectroscopy and find a reason why μ-nitrido complexes have strictly different chemical behaviour to mononuclear and other μ-bridged iron phthalocyanine complexes. The results of spectroscopic experiments were compared with those of multiple scattering simulations (MS) and ground state DFT calculations.

Experimental Results

X-ray spectroscopic experiments were performed at the ID26 beamline. Energy of the incoming beam was selected by means of a pair of Si crystals with a (220) orientation. Higher harmonics were suppressed by three mirrors operating in total reflection Conventional total fluorescence yield (TFY) XANES at Fe K-edge was measured in standard geometry (45 degrees with respect to the incident beam and 45 degrees with the detector) using Silicon diode as a detector. High energy-resolution emission detection was performed using one spherically bent Si (531) analyzer crystal (R=1000 mm). XES spectra at Kβ main and Kβ satellite lines of iron were recorded by setting the incident energy at 7160 eV. The data were normalized by a total spectral area. Spin-selective XANES at Fe K-edge were recorded by setting the emission energy on the maxima of $K\beta_{1,3}$ (7059 eV, spin-down transition) and Kβ' (7045 eV, spin-up transition) emission lines, respectively. RIXS 2D map was measured in the pre-edge and main edge region. In order to limit radiation damage, the samples in the form of 5 mm pellets were cooled down to 30-40 K in the cryostat. Preliminary radiation damage tests were carried out in order to measure maximal exposure time for each sample. If it was necessary to acquire the data for longer times, the samples were moved to a new position with the respect to the beam and measurements were continued. Simulations of conventional XANES and valence-to-core XES spectra were done in the framework of multiple scattering (MS) using a muffin-tin approximation for the shape of potentials of atoms included in the cluster using FEFF8.10 software. The Hedin – Lunquist potential was applied for the exchange interaction with 0.6 eV convolution width.

Conventional (TFY) XANES

TFY Fe K-edge XANES spectra of **1**, **2a, b, 3**, and **4** and their MS simulations are presented in Figure 2. A significant differences were observed between the positions and intensities of pre-edge and main edge features of all four solids. The pre-edge features can be assigned to a dipole-forbidden but quadrupole-allowed 1s→3d transitions. However for non-cubic complexes, dipole intensity mechanism might be prevailing, due to admixing of ligand p-orbitals to the d-levels of iron (the last effect is symmetry-forbidden in the complexes with Oh symmetry). The rising part of XANES curve at higher energies corresponds to 1s → 4p orbital transition of iron.

The pre-edge peak observed in the mononuclear **1** complex is typical for the octahedral or square-pyramidal Fe(III) compounds.[15] The local geometry around Fe(III) site in **1** is square-pyramidal (C_{4v}) due to chloride anion located at the axial position. Formation of the μ-nitrido dimer **3** leads to a strong increase of

pre-edge intensity as compared to the monomer. At the same time the pre-edge feature is shifted to higher energy by ca 0.6 eV. As for the main edge, it does not move significantly compared to the one of monomer **1** but becomes broader. The increase of the pre-edge intensity and its shift are consistent with the increase of oxidation state of iron from Fe(III) in **1** to Fe(III)-N-Fe(IV) in **3**. If purely quadrupole transition is considered, increase in the formal oxidation state of iron should increase the number of free d-orbitals and probability of 1s→3d electron transition. However, another and probably more important effect could be related to introduction of closely staying μ-nitrido ligand. Available in literature Fe-μN distances in μ-nitrido diiron complexes are in the range of 1.63 – 1.67 Å. Bridging nitrogen atom would strongly boosts the dipole mechanism of pre-edge intensity increase due to a strong overlapping of nitrogen orbitals with d-orbitals of iron. An increase in the pre-edge energy position of **3** in comparison with **1** also reflects an increase of the efficient positive charge on iron ion resulting in a stronger electron bonding. The magnitude of the effect observed is consistent with our earlier works on Fe K pre-edge position vs. oxidation state in similar systems. μ-oxo dimers **2a** and **2b** demonstrate lower intensity and lower energy positions of pre-egde peak in comparison with μ-nitrido dimer **3**, in agreement with Fe(III) oxidation state and longer distances between iron and axial oxygen (around 1.75 – 1.80 Å).

Oxidized μ-nitrido dimer **4** exhibits a decrease of the pre-peak intensity and a shift of its center of mass toward higher energies as compared to **3**. The decrease of the pre-edge intensity from neutral **3** to cationic **4** must be related to complex symmetrization leading to a concomitant decrease of the ligand-induced dipole intensity mechanism. At the same time a doublet structure of the pre-peak of **4** becomes resolved. It happens probably because of the loss of the one unpaired electron leaving only the orbitals with paired electrons and the empty ones. By contrast, in the neutral **3** multiplet interactions might be important due to the presence of one unpaired electron on the d-levels.

XANES spectra simulated by FEFF reproduce quite well the qualitative differences between the compounds studied, in particular, they show higher intensity of pre-edge peak for **3** and **4** compared to **2a** as well as positive energy shift (Fig. 2b). However, fine details of pre-edge features could not be resolved probably due to intrinsic limitations of the MS approach. Thus, simulated spectra for **1** and **2a** demonstrate pre-edge shoulders instead of well-distinguished peaks. The pre-peak doublet cannot be seen in the XANES spectrum of oxidized μ-nitrido dimer **4** and its intensity is also not correctly predicted. Overall, XANES spectra confirm significant difference in the electronic structure of iron in **3** and **4** compared to **1** and **2**, which is consistent differences in their chemical activity.

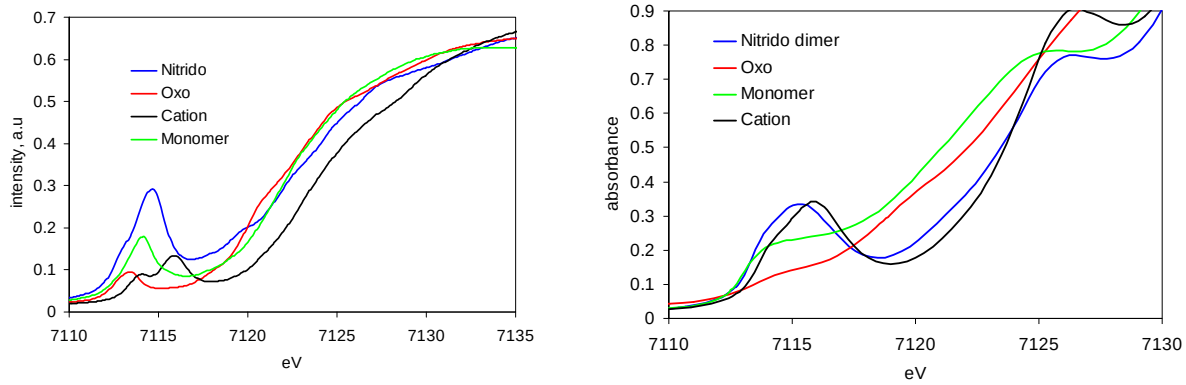

Figure 2 TFY XANES at Fe K-edge of iron complexes: a – experimental data; b- FEFF simulation.

High resolution XES

Kβ satellite lines

Kβ satellite lines corresponding to valence-to-core transitions are obviously sensitive to the chemical state of iron centers in studied complexes. The spectral intensity of these lines is mainly related to the occupancy of iron 4p and ligand np and ns (n=2, 3) orbitals. The experimental valence-to-core spectra of studied compounds are shown in Fig 3a. The Kβ'' or 'cross-over' peak at lower emission energies can be distinguished only for μ-nitrido dimers **3** and **4**. In contrast, for mononuclear **1** and μ-oxo dimers **2** no cross-

over peak but only $K\beta_{2,5}$ feature near the Fermi energy level is observed. Again, μ-nitrido compounds **3** and **4** show different properties compared to **1** and **2**. The Kβ'' peak in 3d metal compounds is assigned to transitions from ligand 2s to metal 1s orbitals [16]. A strong (exponential) dependence of cross-over intensity on the metal-ligand distance was demonstrated [17]. Therefore we suppose that the presence of crossover peak in **3** and **4** is due to short Fe-μN distance (~1.66 Å).

MS simulated spectra reproduce the main differences between valence-to-core spectra of studied complexes and corroborate correlation between the intensity of crossover peaks Kβ'' and the presence of a short metal-ligand bond (Fig 3b). FEFF simulations predict considerable intensity of Kβ'' feature for μ-nitrido dimers **3** and **4**, much weaker feature for μ-oxo complexes **2** and its absence for the monomeric **1**.

The spectra of μ-nitrido dimers **3** and **4** show considerably narrower peaks than other compounds under study, which can be explained by low-spin character of these complexes. It can be qualitatively speculated that the broadening of $K\beta_{2,5}$ feature is due to the multiplet effects, which are obviously more important in the high–spin systems. Further chemically relevant interpretation of $K\beta_{2,5}$ feature is hampered by excessive complexity of many-electron transitions.[18].

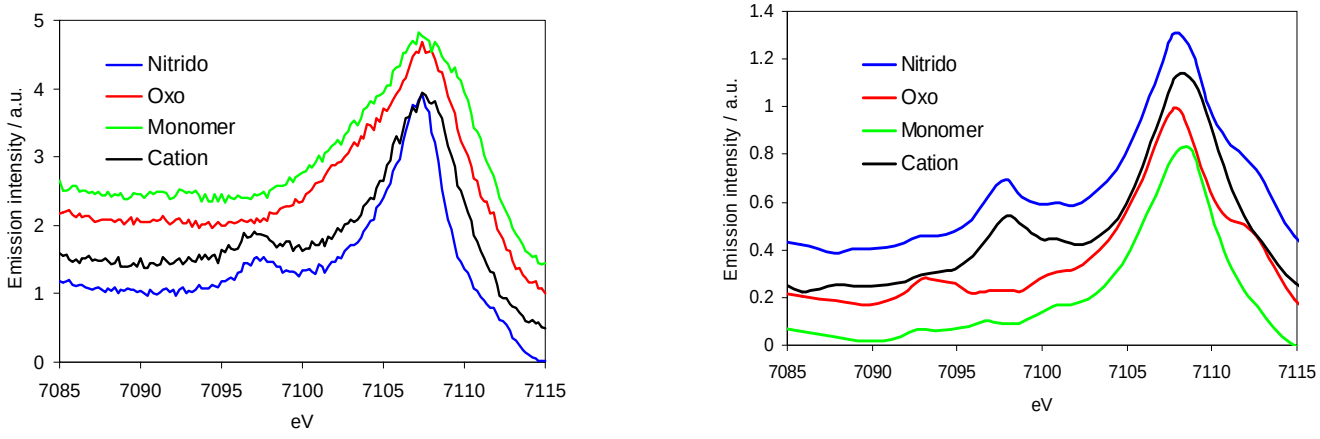

a b

Figure 3 Experimental (a) and calculated (b) Kβ satellite lines (valence-to-core XES) of iron complexes.

Kβ main lines

In the high-spin Fe(III) compounds, having five unpaired 3d electrons (S = 5/2), the Kβ main line splits into multiplets composed of a main $K\beta_{1,3}$ peak near 7058 eV and an intence Kβ' satellite at lower energies. The intensity of Kβ' satellite is proportional to the average spin number of iron [19]. The Kβ main lines of four complexes are presented in Fig. 4. Both neutral **3** and oxidized **4** μ-nitrido dimers show very similar spectra typical for low-spin compounds in which the Kβ' feature has low intensity and is reduced to a low energy shoulder of the main $K\beta_{1,3}$ peak. By contrast, **1** and **2** complexes show XES spectra having intense Kβ' features. There is a strong similarity between Kβ main lines of monomer **1** and μ-oxo dimer **2** confirming a high-spin state of iron in both compounds.

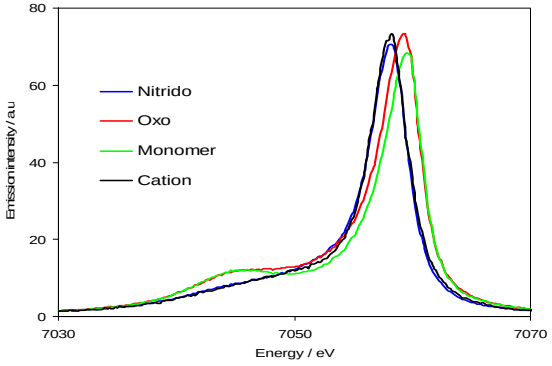

Figure 4. Kβ main XES lines of iron complexes

RIXS and spin-selective XANES

Further information of the iron electronic state of complexes was obtained by RIXS and spin-selective XANES. In the RIXS experiments, the states at the edge of an absorption spectrum are resonantly excited and emission due to their decay is detected [20]. The RIXS final state configurations are $3p^5 3d^{n+1}$ with a core hole in 3p shell and an additional electron in a 3d orbital. Therefore the intensity of transitions strongly depends on the 3d configuration. The strong interaction between an unpaired 3p electron and the valence shell spin can be used to record spin-selective XANES at the Fe K-edge as it was explained in [21,22].
Spin-selective XANES spectra and RIXS 2D maps were measured for all studied complexes (Fig. 5 and 6).

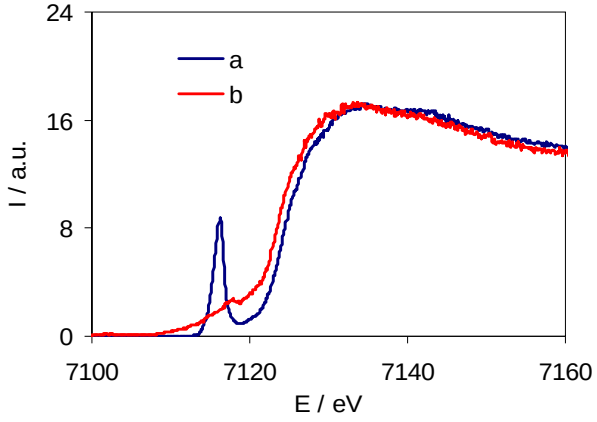

Monomer **1**

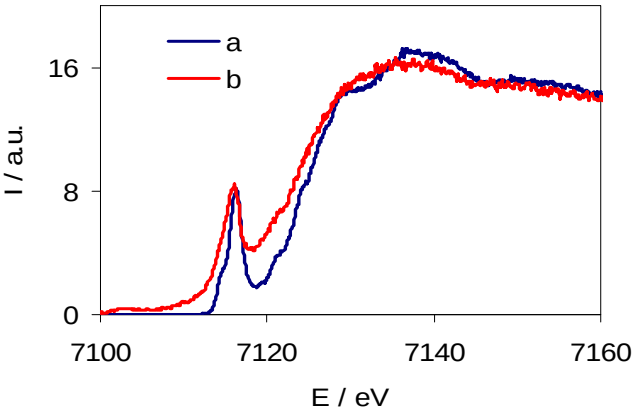

Nitrido dimer **3**

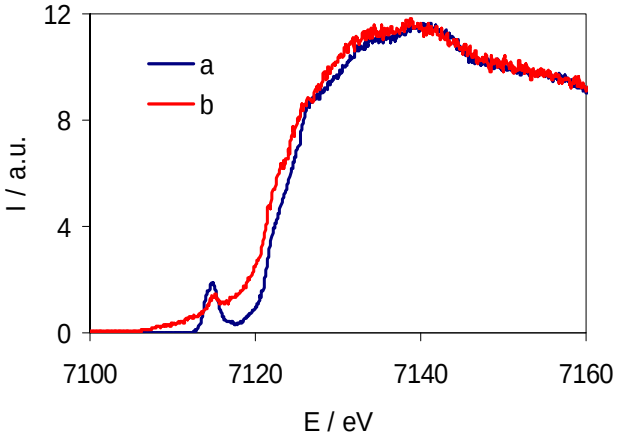

Oxo-dimer **2 a, b**

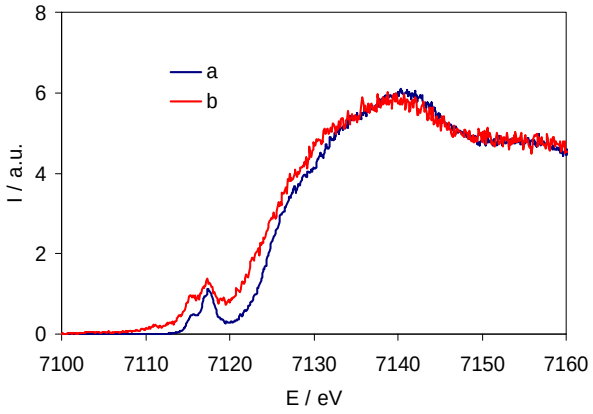

Cation **4**

Figure 5 Spin-selective XANES detected at Kβ' (a) and $K\beta_{13}$ (b) emission energies.

Spin selective XANES (Fig. 5) was obtained by registering the spectra at fixed emission energies corresponding to the maxima of $K\beta_{1,3}$ and Kβ' lines. Data on the Fig. 6 demonstrate almost complete suppression of pre-peak in the Kβ'-excited spectra of monomer **1** and μ-oxo dimer **2**. It means that in this case the spin density on the 3d-levels is high and the electron can be excited only in one spin state, antiparallel to the spin of 3d-shell. In contrast, for μ-nitrido dimers **3** and **4** the pre-peak intensity is the same using Kβ' and $K\beta_{1,3}$ detection energies. These results signify the presence of empty d-levels in the initial state of iron centers, therefore an electron can be excited both in spin-up and spin-down states. Moreover, similar intensity of pre-edge features using Kβ' and $K\beta_{1,3}$ detection energies indicates that d-electron has nearly equal probability of spin-up and spin-down excitation, i.e. it can be excited mostly to the empty levels in the low-spin configurations of Fe(III) and Fe(IV). The bi-dimensional RIXS maps (Fig. 6) provide us

further evidence of this point, showing a striking difference between spectra of low-spin μ-nitrido dimer **3** and its oxidation product **4** on the one side and high-spin μ-oxo dimer **2** and mononuclear **1** on the other. Indeed, for **3** and **4** there is a strong intensity protruding downwards along from the non-resonant pre-edge spot, corresponding to Kβ' emission energy. The appearance of Kβ' intensity after resonant excitation is a proof for the existence of unoccupied levels in the Fe 3d density of states. Therefore, analysis of RIXS maps lead to the same conclusions as spin-selective spectra, but support them on the basis of the bi-dimensional data massive excluding any error of measurement.

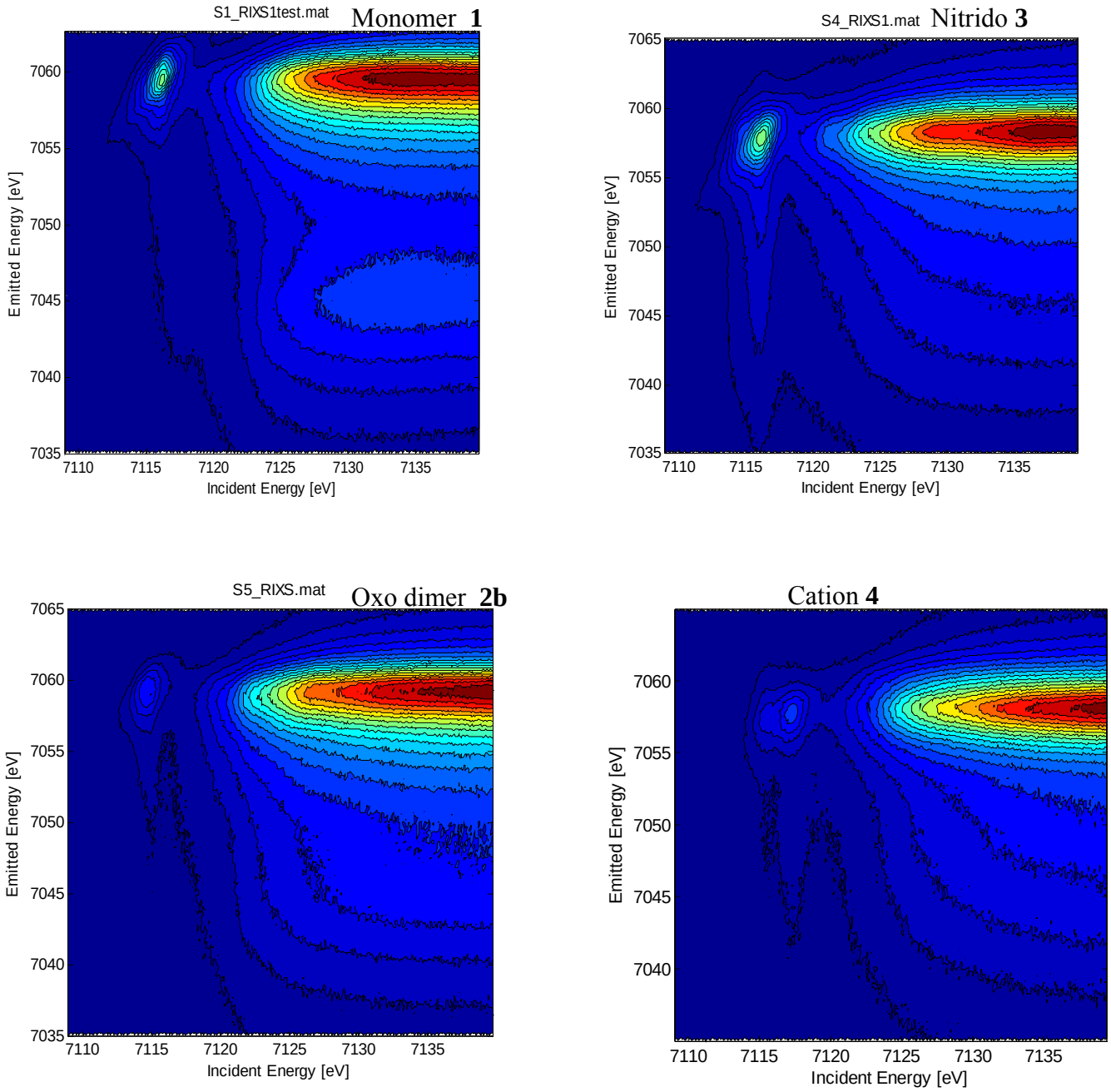

Figure 6 RIXS 2D maps of the studied iron complexes.

Conclusions

In summary, a series of phthalocyanine dimers, bearing a common core Fe-X-Fe (X = N, O) were studied by conventional X-ray absorption near edge spectroscopy (XANES) and high energy-resolution X-ray spectroscopy at Fe K-edge, including X-ray emisson spectroscopy, and resonant inelastic X-ray stattering. It has been demonstrated that Fe(III)-O-Fe(III) core contains locally high spin (S=5/2) antiferromagnetically coupled iron centers. In contrast, in neutral nitrido dimer Fe(III)-N-Fe(IV) iron atoms are in the low spin

states (S=0 and S=1/2). Oxidation of neutral nitrido dimer with bromine produces cation with Fe(IV)-N-Fe(IV) core that does not change significantly the spin state of iron atoms whereas X-ray spectroscopy witness increase of its formal oxidation state. The spectroscopic data agree with the results of ground state DFT calculations and multiple scattering simulations.

FePc dimers and oligomers are known since several decades [23]. However their usefulness for catalysis has been realized only recently [24,25]. In this study we show that chemically similar μ-oxo- and μ-nitrido-dimers show strikingly different electronic properties, which are correlated with the differences in their catalytic activity. The key point of remarkable properties of μ-nitrido- dimers in oxidation catalysis seems to be related to the presence of an unpaired electron on the relatively high orbital of iron, which can be easily withdrawn by an appropriate oxidation agent (H_2O_2, MCPAB). This one–electron event leads to formation of high valent iron species, which can be further involved in the catalytic cycle. The results presented provide an insight into the unusual reactivity of nitride dimer: exceptional stability of the S=0 cation makes easy oxidation towards Fe(IV)Fe(IV) state, thus triggering the catalytic cycle.

References

[1] A. B. Sorokin, E. V. Kudrik, D. Bouchu, *Chem. Commun*. **2008**, 2562.

[2] A. B. Sorokin, E. V. Kudrik, L. X. Alvarez, P. Afanasiev, J. M. M. Millet, D. Bouchu, *Catal. Today* **2010**, doi :10.1016/i.cattod.2010.02.007.

[3] E. V. Kudrik, A. B. Sorokin, *Chem. Eur. J.* **2008**, *14*, 7123.

[4] Ü. İşci, P. Afanasiev, J. M. M. Millet, E. V. Kudrik, V. Ahsen, A. B. Sorokin, *DaltonTtrans.* **2009**, 7410.

[5] B. Floris, M. P. Donzello, C. Ercolani, in *Porphyrin Handbook*; vol. 18 (Eds.: K. M. Kadish, K. M. Smith, R. Guilard) Elsevier Science, San Diego, **2003**, pp 1-62.

[6] L. Shu,, J.C. Nesheim, K. Kauffmann, E. Münck, J.D. Lipscomb, L. Que, Jr. *Science* **1997,** *275*, 515.

[7] P. Afanasiev, D. Bouchu, E. V. Kudrik, J. M. M. Millet, A. B. Sorokin, *DaltonTtrans.* **2009**, 9828.

[8] T. A. Jackson, J. U. Rohde, M. S. Seo, C. V. Sastri, R. DeHont, A. Stubna, T. Ohta, T. Kitagawa, E. Münck, W. Nam, L. Que, Jr. *J. Am. Chem. Soc.*, **2008**, *130*, 12394.

[9] A. Mijovilovich, W. Meyer-Klaucke, *J. Synchr. Rad*. **2003**, *10* 64 .

[10] Shearer J, Scarrow RC, Kovacs JA *J. Am. Chem. Soc* **2002,** *124* , 1709.

[11] Xin Sheng, John H. Horner and Martin Newcomb *J. Am. Chem. Soc.*, **2008**, *130* , 13310.

[12] A. Arcovito, M. Benfatto, M. Cianci, S.S. Hasnain, K. Nienhaus, G.U. Nienhaus, C. Savino, R. W. Strange, B. Vallone, S. Della Longa, *Proc. Natl. Acad. Sci. U.S.A.* **2007,** *104*, 6211.

[13] S A Suchkova, A Soldatov, K Dziedzik-Kocurek, M J Stillman, *J. Phys. Conf. Ser.* **2009**, *190*, 012211

[14] Heijboer WM, Glatzel P, Sawant KR, Lobo RF, Bergmann U, Barrea RA, Koningsberger DC, Weckhuysen BM, de Groot FMF *J. Phys. Chem*. B **2004**, 108, 10002

[15] C. Cartier, M. Momenteau, E. Dartyge, A. Fontaine, G. Tourillon, A. Michalowicz, M. Verdaguer, *J. Chem. Soc. Dalton Trans.* **1991**, 609.

[16] D.S. Urch, Electron spectroscopy: Theory, Techniques, and Applications. in: C.R. Brundle, A.D. Baker, Eds., Academic Press, New York, **1979**, vol. 3, pp. 1–39.

[17] U. Bergmann, C.R. Horne, T.J. Collins, J.M. Workman and S.P. Cramer. *Chem. Phys. Lett.* **1999,** *302,* 119.

[18] M. Deutsch, O. Gang, K. Hämäläinen and C.C. Kao. *Phys. Rev. Lett.* **1996,** *76,* 2424.

[19] J. Badro, V.V. Struzhkin, J.F. Shu, R.J. Hemley and H.-K. Mao, *Phys. Rev. Lett.* **1999,** *83,* 4101..

[20] A. Kotani and S. Shin. *Rev. Mod. Phys.* **2001,** *73,* 203.

[21] G. D. Pirngruber, J.D. Grunwaldt, J.A. van Bokhoven, A. Kalytta, A. Reller, O. V. Safonova, P. Glatzel *J. Phys. Chem. B*, **2006,** *110,* 18104.

[22] Wang, X.; Randall, C. R.; Peng, G.; Cramer, S. P. *Chem. Phys. Lett.***1995**, *243*, 469.

[23] N Kobayashi *Coord. Chem. Rev.* **2002,** *227,* 129.

[24] A. B. Sorokin, S. Mangematin, C. Pergrale *J. Molec. Catal. A* **2002,** *182-183*, 267.

[25] C. Pergrale, A. B. Sorokin *C. R. Acad. Sci. Ser. IIC* ***2000,*** *3, 803-810*